Supporting Information For:

Simultaneous Adsorption and Electrochemical Reduction of N-Nitrosodimethylamine using Carbon-Ti$_4$O$_7$ Composite Reactive Electrochemical Membranes

Soroush Almassi[§], Zhao Li[†], Wenqing Xu[†], Changcheng Pu[+], Teng Zeng[+], and Brian P. Chaplin[§*]

[§]Department of Chemical Engineering, University of Illinois at Chicago, 810 S. Clinton St., Chicago, IL 60607

[†]Department of Civil and Environmental Engineering, Villanova University, 800 E. Lancaster Ave., Villanova, PA 19085

[+]Department of Civil and Environmental Engineering, Syracuse University, 151 Link Hall, Syracuse, NY 13244

*Corresponding author at: Department of Chemical Engineering, University of Illinois at Chicago, Chicago, IL 60607, USA

E-mail address: chaplin@uic.edu (Brian P. Chaplin)

Phone No.: +13129960288

Pages: 22

Figures: 12

Tables: 5

1) REM Synthesis.

The Ti_4O_7 powder was synthesized by the reduction of 5.0 g of TiO_2 powder in the presence of 1.0 atm flowing H_2 gas at 1050 ºC for 6 h in a tube furnace (OTF-1200X, MTI, Richmond, CA). The Ti_4O_7 REMs were synthesized by mixing 0.6 g Ti_4O_7 powder with 2-3 wt% paraffin oil as a binder. The powder and binder were mixed using mortar and pestle for 20 min. The mixture was placed in a 1.12 cm diameter die and a uniaxial pressure of ~7 bar was applied by a hydraulic press (RAMCO, Kent, WA). The pellets were sintered in a tube furnace for 6 h in the presence of 1.0 atm Ar at 1050 °C.

The carbon-Ti_4O_7 composite REMs were synthesized to increase the adsorption capacity of NDMA. For the synthesis of MWCNT-Ti_4O_7 REMs, 0.54 g of Ti_4O_7 powder was combined with an appropriate amount of dimethylformamide (DMF) for making a 6 wt% solution, which was dispersed using a sonicator (Model: 08895-38, Cole-Parmer, Vernon Hills, IL) for 2 h. A second solution containing MWCNTs (0.06 g) in DMF (3 wt%) was sonicated for 15 min. The two solutions were combined and then sonicated for 3 h.[1] The solution was filtered through a 0.2 μm polyvinylidene fluoride (PVDF) membrane and then dried in a convection oven for 8 h at 200 °C. For synthesizing PAC-Ti_4O_7 phase REMs, 0.54 g Ti_4O_7 powder and 0.06 g PAC were added to 15 mL of DI water. The slurry was sonicated for 30 min and then filtered through a 0.2 μm PVDF membrane. The powder was dried at 100 °C for 3 h. The carbon-composite REMs were synthesized by identical methods as described above for the Ti_4O_7 REM, but with using the blended powders.

2) Flow-through Reactor.

An upflow, electrochemical, flow-through reactor was used for adsorption and electrochemical oxidation or reduction of NDMA. The solution first passed through the working electrode followed by the counter electrode. A schematic of the reactor setup is shown in Figure S-1. All experiments employed a three-electrode setup and were carried out with either the REM, MWCNT-REM, or PAC-REM with 0.5 cm^2 surface area as the working electrode (cathode), a 0.33 cm^2 surface area 316 stainless steel tube as the counter electrode (anode), and a leak-free 1 mm diameter Ag/AgCl as the reference electrode (LF-100, Warner Instruments, Hamden, CT). The interelectrode gap between the working and reference electrodes was ~1 mm and between working and counter electrodes was ~ 3mm. A digital gear pump (Model No. 75211-70, Micropump, Vancouver, WA) was used to control the permeate flux. Potentials and currents were applied and measured using a Gamry Interface 1000 potentiostat/galvanostat (Gamry Instruments, Warminster, PA), and all potentials were reported versus the standard hydrogen electrode (/SHE) and were corrected for the solution resistance between the working and reference electrodes, which was determined by EIS. The permeate flux was held constant at either 100 or 200 L m^{-2} h^{-1} (LMH), which gave a liquid residence time in the REMs of either 22 or 11 s, respectively.
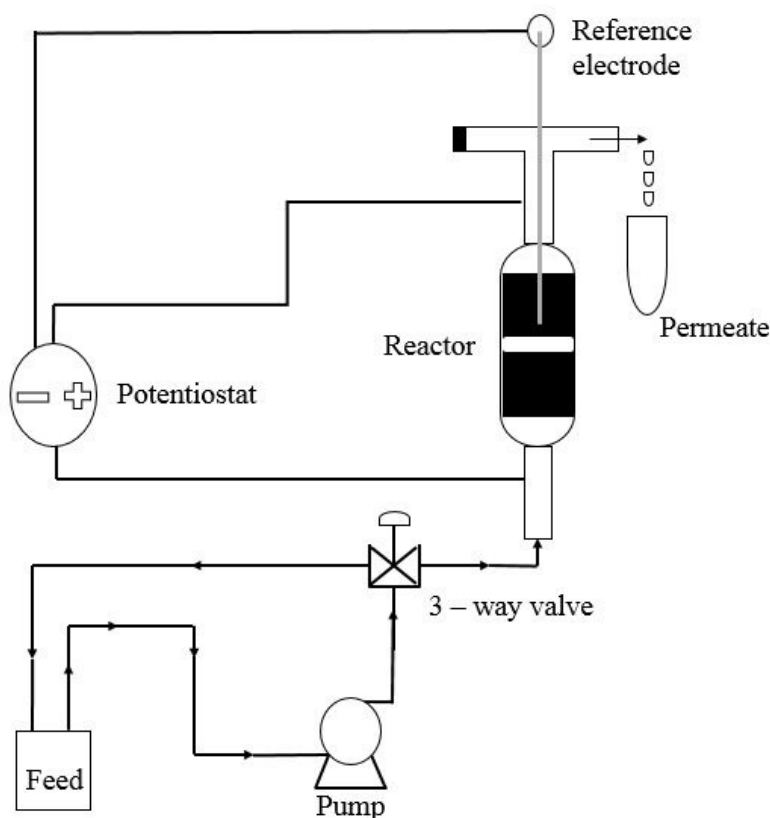

Figure S-1. Schematic of experimental flow-through reactor setup.

3) Batch Experiments

To determine the enthalpy of activation ($\Delta H^{\ddagger}$) for electrochemical NDMA reduction at -1.12 and -1.47 V/SHE, batch experiments were carried out in a jacketed 100 mL divided cell reactor using a rotating disk electrode (RDE). A Nafion A115 membrane (Ion Power, Inc., New Castle, DE) was used to separate anode and cathode components. Experiments were conducted using a three-electrode setup with 0.35 cm^2 Ti$_4$O$_7$ REM as working electrode (cathode), Pt wire as counter electrode, and Ag/AgCl reference electrode. The REM was placed in the RDE and rotated at 5000 RPM. The Ag/AgCl reference electrode was placed 5 mm from the working electrode. Both working and reference electrodes were placed in a chamber that was filled with 150 μM NDMA and 10 mM NaH$_2$BO$_3$. The counter electrode was a Pt wire (Alfa Aesar, Tewksbury, MA) and was placed in the anode chamber, which was filled with 10 mM NaH$_2$BO$_3$. The reactor temperature was controlled at either 15, 20, 25, or 30 °C using a recirculating water bath (NESLAB RTE 7, Thermo Fisher Scientific, Grand Island, NY). The desired cathodic potential was applied using a Gamry Interface 1000 potentiostat/galvanostat. The reaction rate constants were determined by regression and the $\Delta H^{\ddagger}$ values were calculated using the Arrhenius equation. To clarify the reduction mechanism of NDMA, an additional experiment was carried out similarly as described above but with an Argon gas purge to remove dissolved oxygen.

4) Analytical Methods

The NDMA concentrations were measured using a Shimadzu UFLC XR HPLC with a Phenomenex Kinetex 5μm C18 column and a photodiode array detector (PDA) (Nexera X2, Shimadzu) (254 nm). The mobile phase was a 55:45 mixture of methanol to DI water at a flow rate of 1 mL min^{-1}. The method detection limit (MDL) was 0.1 μM for NDMA. The NDMA concentrations of select samples were analyzed using gas chromatography-mass spectroscopy (GC-MS) (Agilent 6890N GC/5973 MSD, USA) or liquid chromatography-mass spectroscopy (LC-MS). The GC-MS analysis was performed with a DB-1701 column (30 m× 0.25 mm, 1μm). Both methods utilized a solid phase extraction (SPE) method. For the LC-MS method, 100 mL samples were spiked with a methanolic solution of NDMA-d6 as the internal standard and extracted using a dual-cartridge solid-phase extraction method. Sample extracts were analyzed using a Dionex UltiMate 3000 high-performance liquid chromatograph interfaced with a Thermo LTQ XL hybrid ion trap-Orbitrap high-resolution mass spectrometer. Selected ion monitoring of NDMA was operated with a nominal resolving power of 15,000 in positive electrospray ionization mode. NDMA was quantified using 7-point calibration curves with reference to NDMA-d6. The method detection limit and method quantification limit were 5 ng/L and 15 ng/L, respectively. The concentration of NO_3^-, NH_4^+, and dimethylamine (DMA) were determined by ion chromatography (IC) (Dionex, ICS-2100). For NO_3^- analysis a Dionex Ion Pac AS18 column, KOH eluent, and 0.75 mL min^{-1} flow rate were used. For NH_4^+ and DMA analysis an Ion Pac CS16 column with 28 mM *methanesulfonic acid* at a 1 mL min^{-1} flow rate was used. The MDLs were 10 μM for DMA and 5 μM for NH_4^+ and NO_3^-. For all liquid chromatographic methods, the analytical standards were prepared in the background electrolytes used in experiments.

All dissolved nitrogen species (except N_2) were oxidized to NO_3^-, which was detected by IC. For evaluating the adsorbed nitrogen species on the REMs after flow-through experiments, all REMs (pristine and used samples) were crushed using mortar and pestle and 0.1 g of the crushed REMs were analyzed for total N in triplicate samples. After oxidation, the samples were filtered through 0.45 μm PVDF syringe filters. Control experiments were conducted with pristine pellets and total N concentrations were below the detection limit (5 μM).

5) Crystal size determination.

Table S-1. REMs crystal size calculation using the Scherrer equation

FWHM (rad)	Theta (deg.)	d (m)
1.46E-03	10.41	9.63E-08
2.62E-03	13.21	5.44E-08
3.67E-03	15.9	3.93E-08
2.80E-03	26.63	5.53E-08
3.22E-03	27.54	4.85E-08
	Average for REM	5.88E-08 ± 1.92E-08

FWHM (rad)	Theta (deg.)	d (m)
2.60E-03	10.36	5.43E-08
2.38E-03	13.17	6.00E-08
2.00E-03	15.85	7.20E-08
5.57E-03	26.58	2.79E-08
3.23E-03	27.5	4.85E-08
	Average for PAC-REM	5.25E-08 ± 1.43E-08

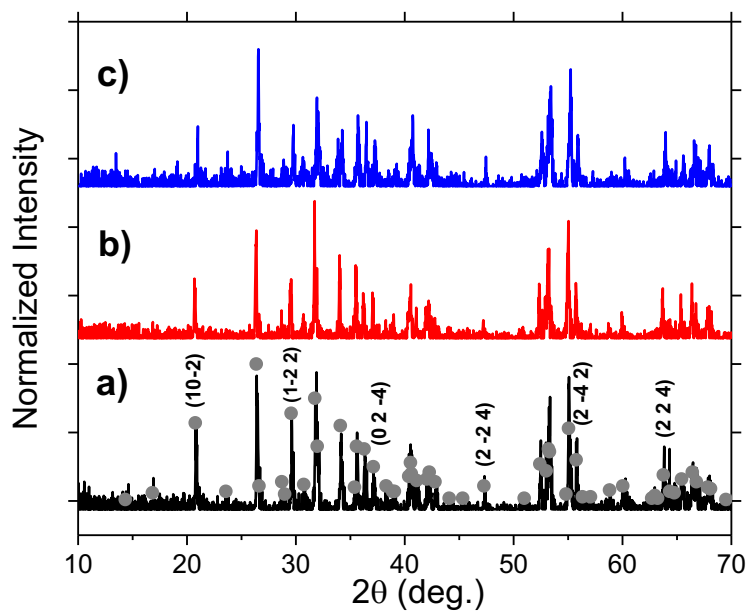| FWHM (rad)	Theta (deg.)	d (m)
1.26E-03	10.45	1.12E-07
2.60E-03	13.27	5.49E-08
6.21E-03	16	2.32E-08
4.57E-03	20.35	3.24E-08
5.81E-03	26.68	2.67E-08
	Average for MWCNT-REM	4.99E-08 ± 3.23E-08

6) XRD Data.

Figure S-2. X-Ray diffraction results of a) REM, b) PAC-REM, and c) MWCNT-REM. Grey points represent the Ti_4O_7 XRD standard peak positions.
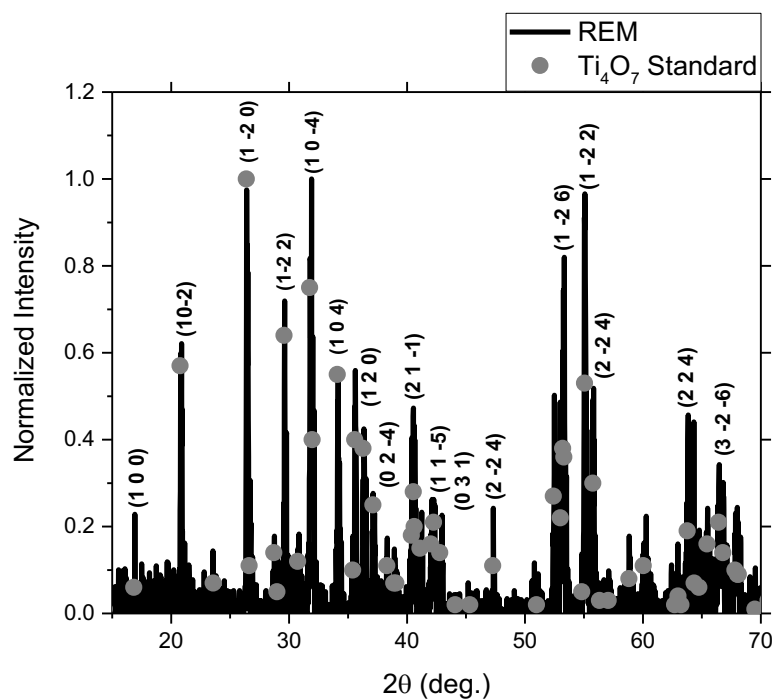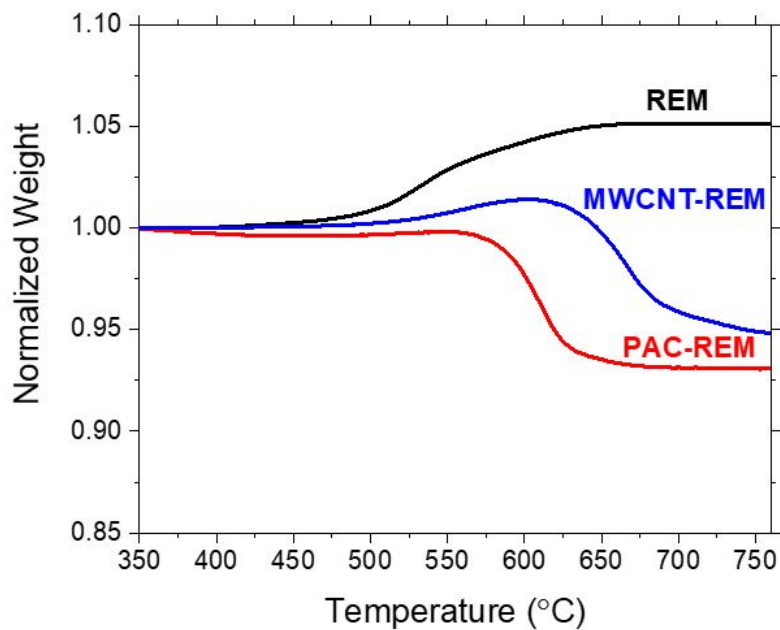

Figure S-3. XRD data for REM. Grey points represent Ti_4O_7 standard peak positions.

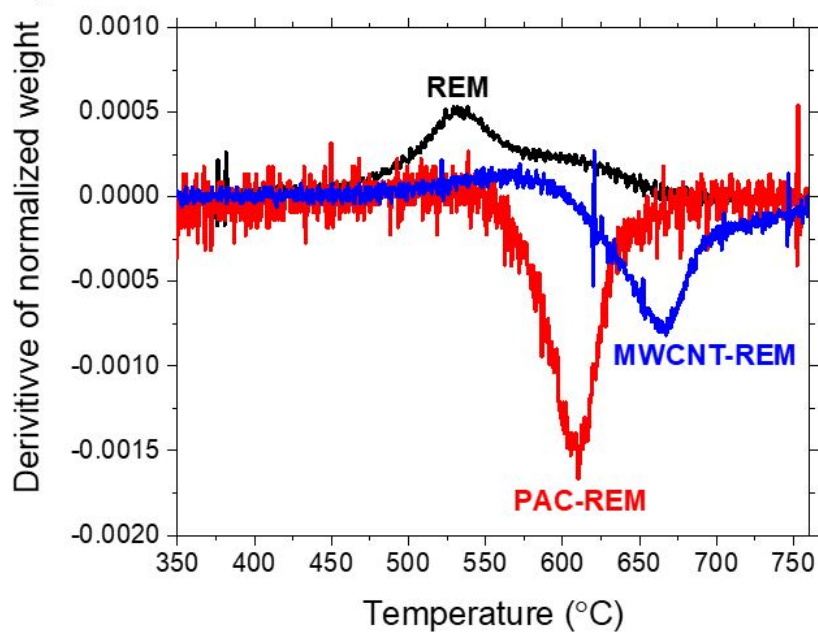## 7) TGA Analysis.

a)

b)

Figure S-4. a) TGA results and b) Differential TGA results of REM, PAC-REM, and MWCNT-REM.

8) Pore size measurement of REMs.

The effective pore size (r) of each REM was measured using the Hagen-Poiseuille equation.

$$v = \frac{r^2 \, \Delta P}{8\mu\Delta x}$$
(S-1)

In this equation, v is the average pore velocity (m s^{-1}), r is the effective pore radius (m), ΔP is the trans-membrane pressure (Pa), μ is DI water viscosity, and Δx is the electrode thickness. The value of r was found by linear regression of v versus ΔP data (Figure S-5). The r values for REM, PAC-REM, and MWCNT-REM were calculated as 0.35 ± 0.05 µm, 0.30 ± 0.04 µm, and 0.20 ± 0.04 µm, respectively.
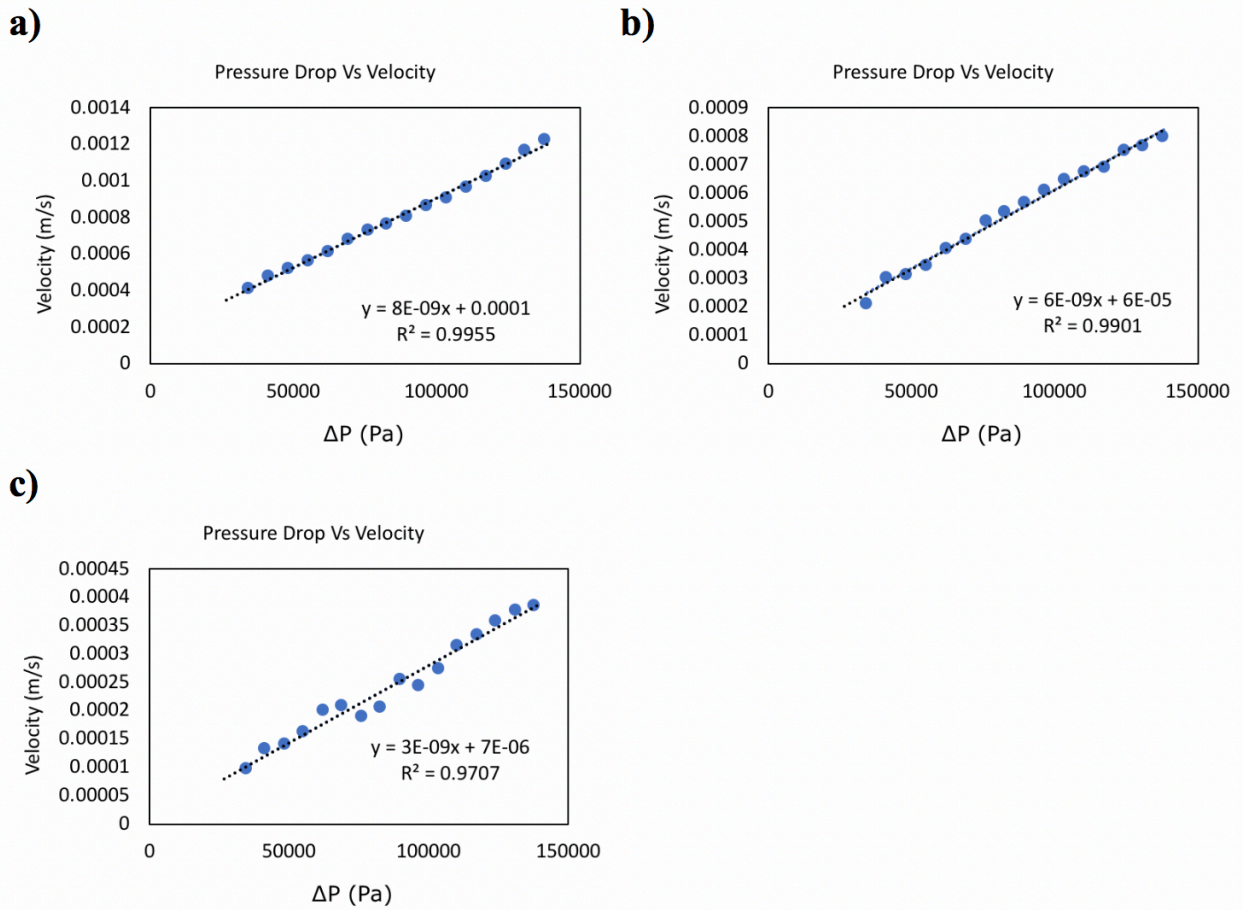
a)

b)

c)

Figure S-5. Pore size measurement using Hagen-Poiseuille equation for: a) REM, b) PAC-REM, and c) MWCNT-REM.

9) Batch Isotherm Results.

A mixture of nitrosamines stock solution (N-nitrosodimethylamine (NDMA), N-nitrosomethylethylamine (NMEA), N-nitrosodibutylamine (NDBA), N-nitrodi-n-propylamine (NDPA), N-nitrosopyrrolidine (NPYR), N-nitrosopiperidine (NPIP), and N-nitrosodiethylamine (NDEA)) in 10 mM K_2HPO_4 (pH 7) was added to borosilicate glass vials containing 0.71 g L^{-1} of pre-weighed Ti_4O_7, PAC-Ti_4O_7, or MWCNT-Ti_4O_7 powder. A series of concentrations of nitrosamines ranging from 0 to 10 mg L^{-1} were prepared. The vials were capped with Teflon-lined septa, placed on an end-to-end rotator at 30 revolutions per minute (RPM) in the dark at 25 °C for 24 hours, which was previously determined to be sufficient to reach equilibrium. All experiments were conducted in duplicate. Samples were collected after 24 hours and centrifuged at 3000 RPM for 15 minutes to separate the aqueous and solid phases.
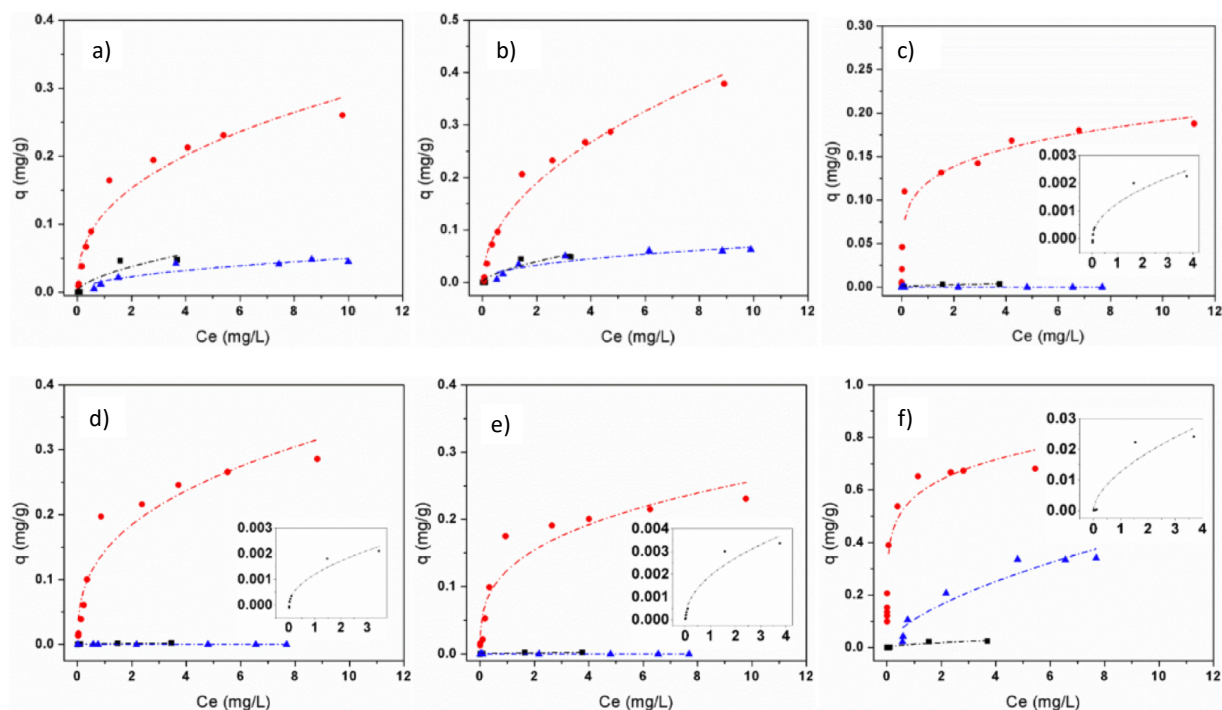

Figure S-6. Adsorption isotherms for nitrosamines onto Ti_4O_7 (black), 10 wt% PAC/Ti_4O_7 (red), and MWCNTs/Ti_4O_7 (blue). Seven nitrosamines include a) NDEA, b) NMEA, c) NPIP, d) NPYR, e) NDPA, and f) NDBA. Data are fit to the Freundlich model: $q = K_F C_e^n$.

Table S-2. Freundlich model parameters (K_F and n) for adsorption of nitrosamines onto Ti_4O_7, PAC/Ti_4O_7, and $MWCNT/Ti_4O_7$ powders.

|	Ti_4O_7			PAC/Ti_4O_7			CNT/Ti_4O_7		
	K_F (mg^{1-n}*L^n/g)	n	R^2	K_F (mg^{1-n}*L^n/g)	n	R^2	K_F (mg^{1-n}*L^n/g)	n	R^2
(A)NDMA	0.026± 0.005	0.634± 0.186	0.890	0.134± 0.011	0.495± 0.046	0.965	0.024± 0.005	0.444± 0.099	0.849
(B)NDEA	0.003± 0.000	0.560± 0.154	0.899	0.073± 0.006	0.344± 0.046	0.928	--	--	--
(C)NMEA	0.025± 0.006	0.596± 0.186	0.876	0.116± 0.010	0.395± 0.048	0.937	0.016± 0.004	0.482± 0.116	0.837
(D)NPip	0.001± 0.000	0.500± 0.097	0.936	0.124± 0.011	0.316± 0.052	0.899	--	--	--
(E)NPyr	0.001± 0.000	0.521± 0.098	0.940	0.144± 0.013	0.362± 0.052	0.916	--	--	--
(F)NDPA	0.002± 0.000	0.484± 0.083	0.948	0.120± 0.008	0.201± 0.033	0.914	--	--	--
(G)NDBA	0.013± 0.003	0.577± 0.164	0.898	0.573± 0.025	0.162± 0.024	0.933	0.107± 0.022	0.616± 0.118	0.906

10) NDMA breakthrough curves.
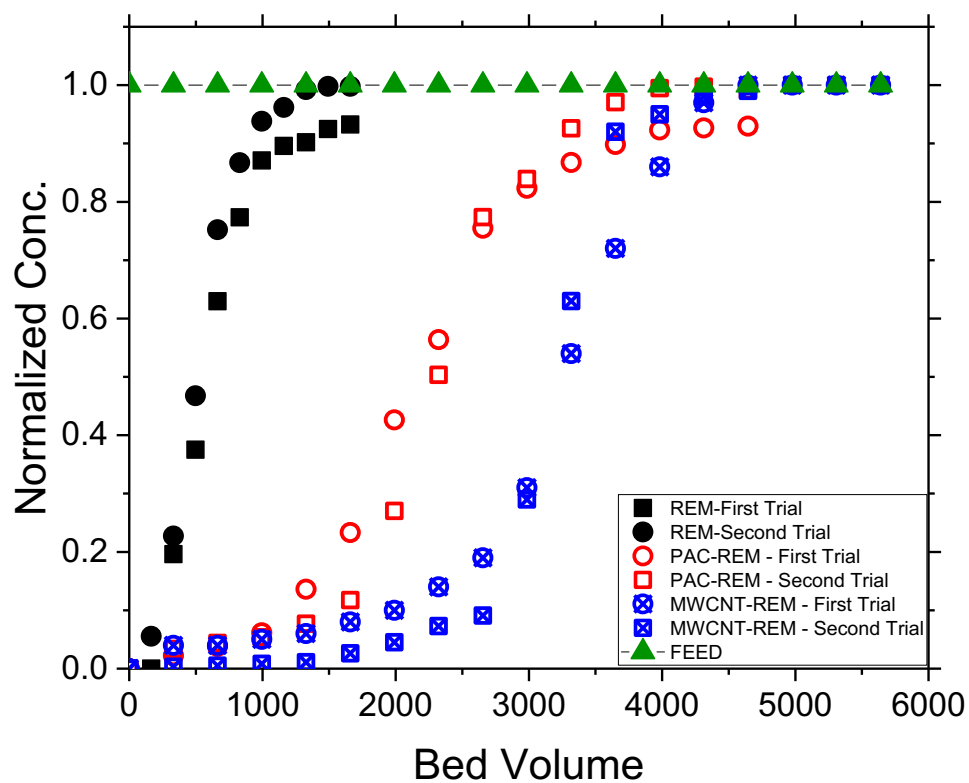
Figure S-7. Breakthrough curves for REMs with initial feed concentration of 10 μM NDMA and 10 mM NaH$_2$BO$_3$ background electrolyte.
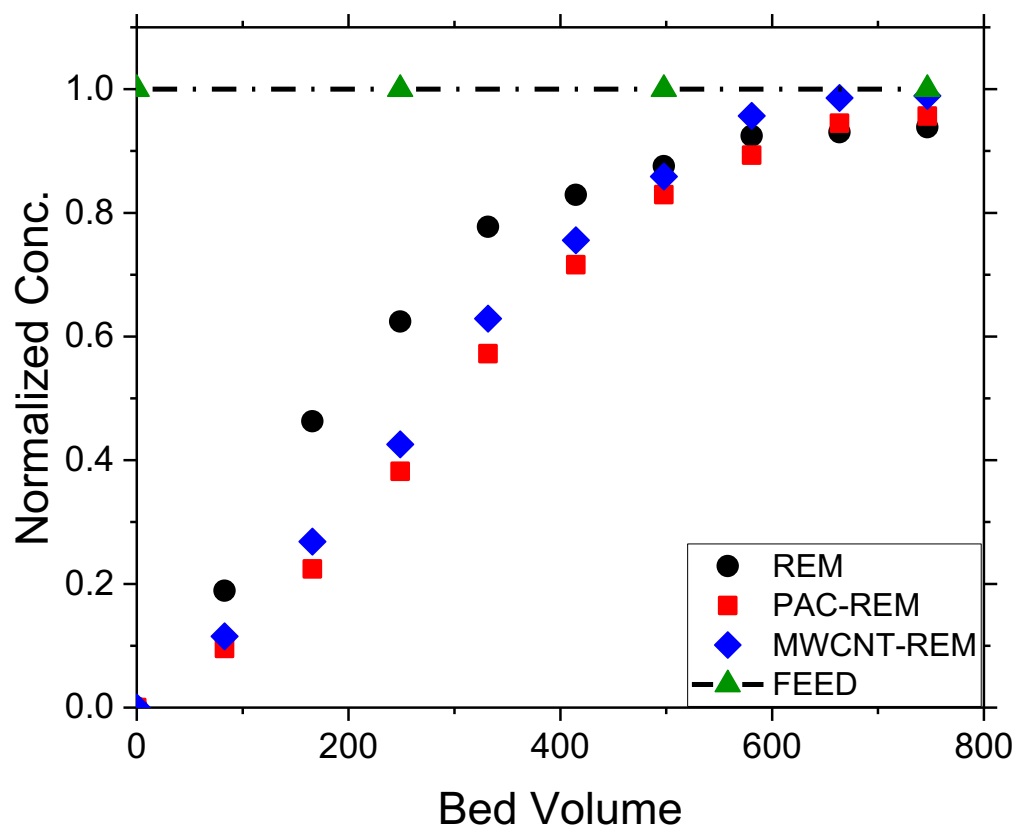
11) Chloride breakthrough curves.

Figure S-8. Breakthrough curves for REMs with initial feed concentration of 1 mM NaCl and 10 mM NaH$_2$BO$_3$ background electrolyte.

12) Analysis of REM Breakthrough curves.

The kinetics of the adsorption process for flow-through experiments can be obtained by analyzing the breakthrough curves using the following equation[2]:

$$\ln\left[\frac{C}{C_o}\right] = \frac{k_a C_0}{q_0\,\rho\,(1-\varepsilon)}t - k_a t_d \tag{S-2}$$

where k_a is the adsorption rate constant (h^{-1}), q_0 is the solute concentration in the saturated adsorbent (determined by batch isotherm results), ρ is the adsorbent density (3700 kg m^{-3}),[3] ε is the bed volume fraction (0.3), t is time (h), t_d is the hydraulic detention time in the pellet, and C and C_o are the permeate and feed concentrations (mg m^{-3}), respectivley. Plots of $\ln\left[\frac{C}{C_o}\right]$ versus t are provided in Figure S-9 and the regression results were used to estimate k_a. The PAC-REM data provided k_a = 7.2 x 10^{-2} ± 1.0 x 10^{-2} s^{-1} for the 10 μM NDMA concentration and k_a = 6.6 x 10^{-2} ± 9.6 x 10^{-3} s^{-1} for the 150 μM NDMA concentration. The MWCT-REM data provided k_a = 1.9 x 10^{-3} ± 2.0 x 10^{-4} s^{-1} for the 10 μM NDMA concentration and k_a = 8.3 x 10^{-4} ± 1.8 x 10^{-4} s^{-1} for the 150 μM NDMA concentration. These results indicated that adsorption kinetics were faster for the PAC-REM compared to the MWCNT-REM. Also, the similar k_a values for the two different feed concentrations for a given material, indicated that adsorption was a first-order process under the concentration range tested in the experiments.

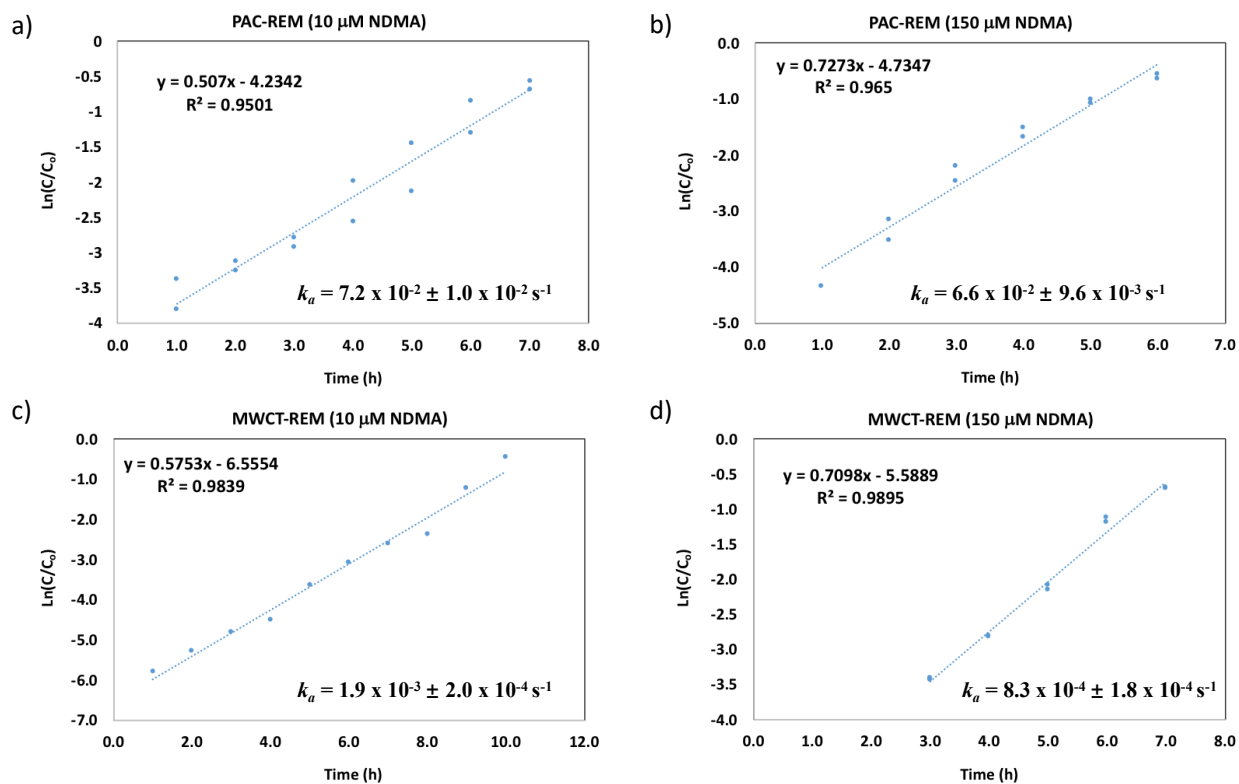**Figure S-9.** Plots of NDMA breakthrough curves for values of C/C_o up to approximately 0.5. a) PAC-REM, 10 µM NDMA; b) PAC-REM, 150 µM NDMA; c) MWCNT-REM, 10 µM NDMA; d) MWCNT-REM, 150 µM NDMA

13) NDMA oxidation results for REMs.

a)
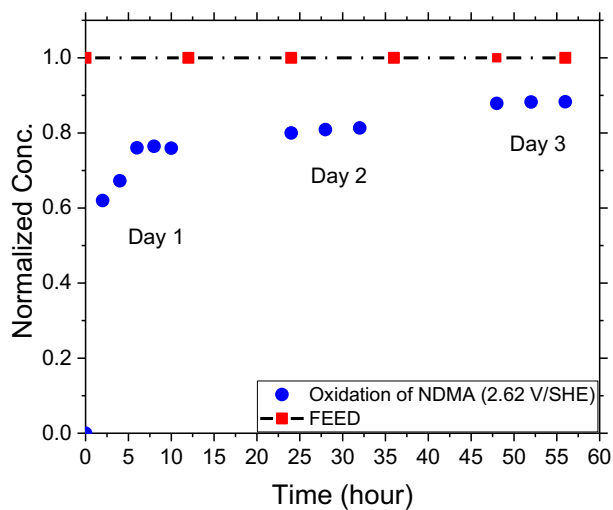
b)
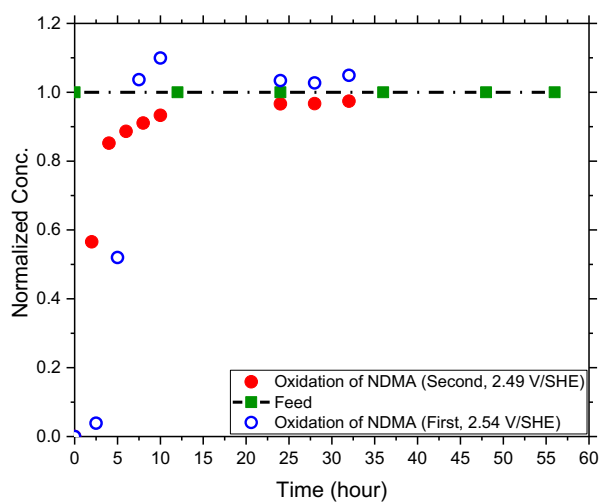
Figure S-10. Oxidation results for REMs tested with 10 µM NDMA feed solution in a 10 mM NaH$_2$BO$_3$ background electrolyte. a) REM, and b) PAC–REM.

14) Surface Water Composition.

Table S-3. Composition of surface water sample.

	Filtered Surface Water
Sodium	0.17 mM
Potassium	0.02 mM
Calcium	0.66 mM
Magnesium	0.38 mM
Chloride	0.35 mM
Sulfate	0.01 mM
Bicarbonate	2.02 mM
Alkalinity	124 mg L^{-1} as $CaCO_3$
COD	11 mg L^{-1}
pH	7.6
Conductivity	283 μS cm^{-1}
Ionic Strength[4]	4.5 mM

15) Activation Energy Determination.

a)

Experimental Temperature = 15 °C

y = -0.000011x - 0.011244
R² = 0.991457

b)

Experimental Temperature = 20 °C

y = -0.000016x - 0.004106
R² = 0.978015

c)

Experimental Temperature = 25 °C

y = -0.000025x + 0.009815
R² = 0.999086

d)

Experimental Temperature = 30 °C

y = -0.000032x - 0.013728
R² = 0.993038

e)

Activation Energy

y = -6382.8x + 10.745
R² = 0.9906

Figure S-11. Batch experimental results for NDMA reduction at a cathodic potential of -1.12 V/SHE on REM at **a)** 15 °C, **b)** 20 °C, **c)** 25 °C, **d)** 30 °C. Solid line represents linear regression. **e)** Determination of activation energy using the Arrhenius equation.

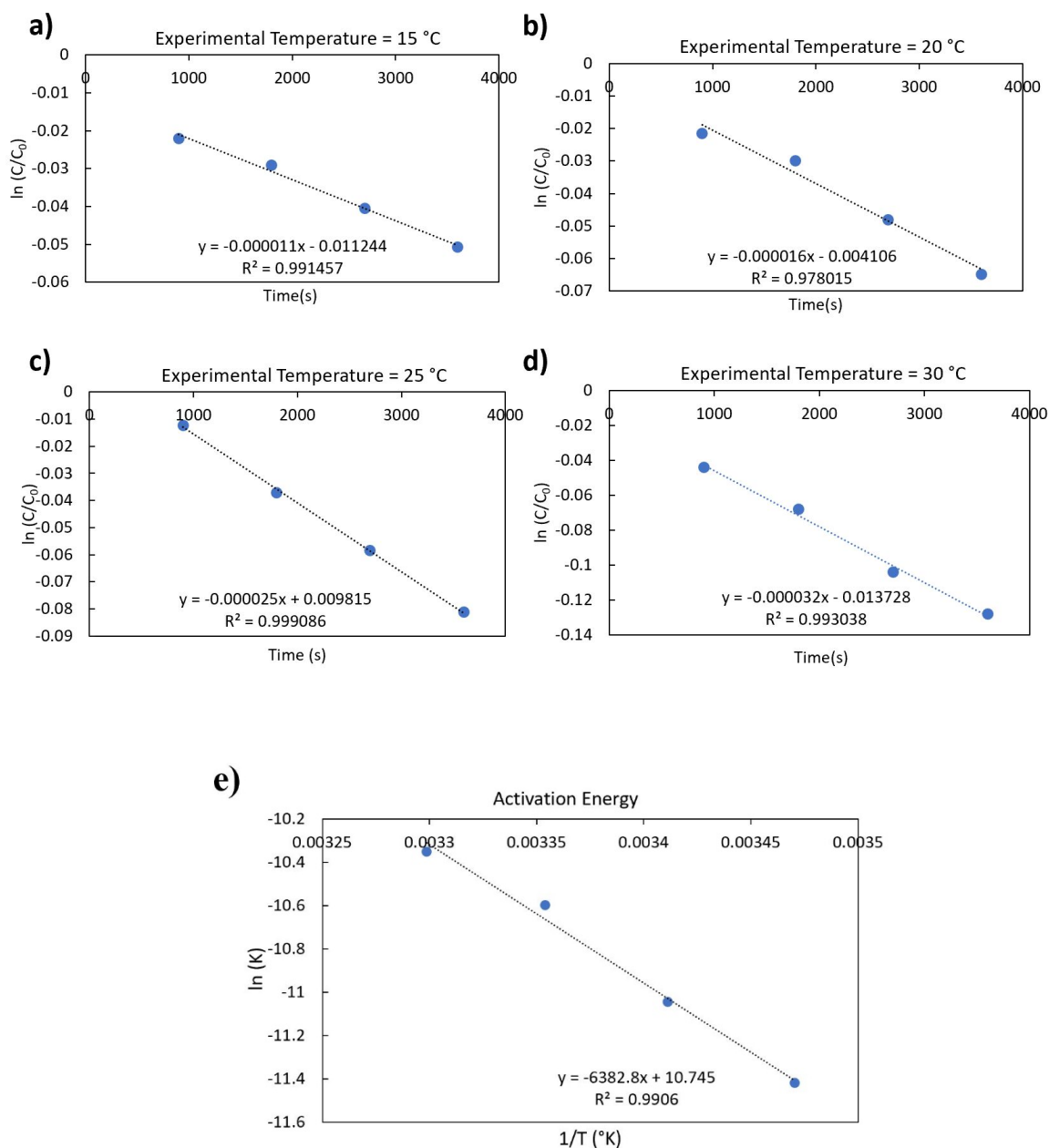**Figure S-12.** Batch experimental results for NDMA reduction at a cathodic potential of -1.47 V/SHE on REM at **a)** 15 ºC, **b)** 20 ºC, **c)** 25 ºC, **d)** 30 ºC. Solid line represents linear regression. **e)** Determination of activation energy using the Arrhenius equation.
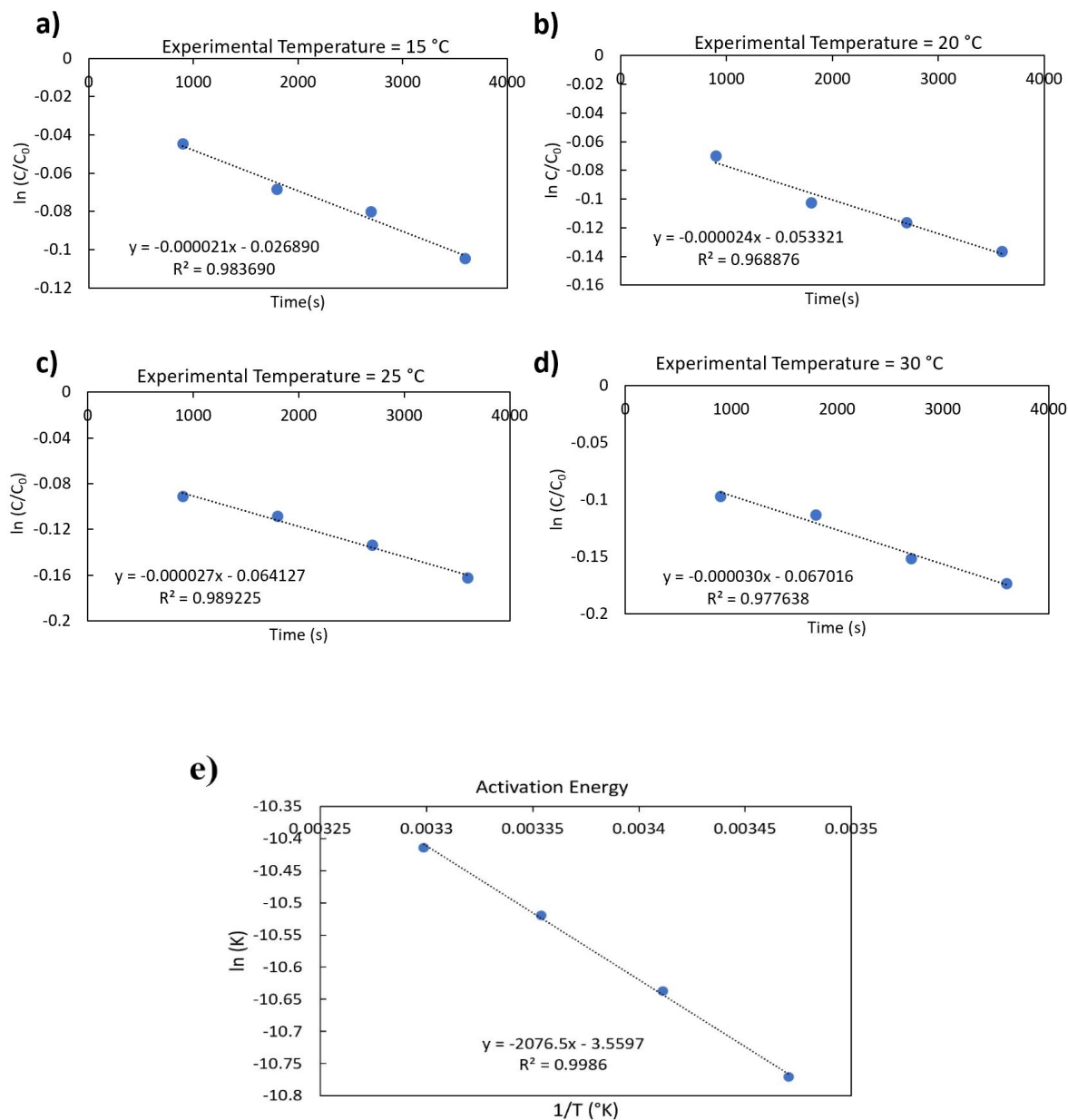
16) Coordinates of DFT Optimized Structures

Table S-4. Atomic positions (in angstroms) of geometric optimized structures using the 6-31-G++d basis set. a) DMA + NO + 3H$_2$O (energy = -494.16144275 Ha); b) [NDMA--2H$_2$O] (energy = -417.18191356 Ha); c) [NDMA--2H$_2$O]$^-$ (energy = -417.28525015 Ha).

a)

Atom	X	Y	Z
N	1.482572	0.051549	0.014638
C	2.051404	1.167589	-0.759973
H	1.257842	1.885659	-0.973283
H	2.839597	1.642253	-0.173837
H	2.460368	0.769101	-1.690075
C	2.482117	-0.971139	0.380389
H	3.245263	-0.508881	1.009152
H	1.978660	-1.768969	0.925945
H	2.927998	-1.356294	-0.538956
N	0.337959	-0.558491	-0.817945
O	-0.249285	-1.418316	-0.086982
O	-1.773211	1.575075	-0.581266
H	-0.998692	1.168562	-1.014262
H	-2.393063	0.816952	-0.497400
O	-2.978901	-0.912498	-0.185941
H	-3.419862	-1.254641	-0.979067
H	-2.057418	-1.251920	-0.233146
H	1.018287	0.416373	0.865588
O	-0.609494	0.839210	1.886759
H	-0.855885	-0.100067	1.825960
H	-1.060814	1.243987	1.113476

b)

Atom	X	Y	Z
N	0.181236	0.936926	0.000017
C	1.281334	1.893096	0.000077
H	2.219885	1.339133	0.000078
H	1.213283	2.517800	-0.893078
H	1.213242	2.517730	0.893279
C	-1.203254	1.397872	0.000005
H	-1.189472	2.486437	0.000034
H	-1.714395	1.028456	-0.893159
H	-1.714424	1.028408	0.893133
N	0.474619	-0.310905	-0.000003
O	-0.488588	-1.103843	-0.000044
O	3.270756	-1.449129	0.000044
H	2.377858	-1.055303	0.000029
H	3.115078	-2.406258	0.000058
O	-3.341704	-1.220258	-0.000080
H	-3.727517	-0.330535	-0.000246
H	-2.376715	-1.067980	-0.000085

c)

Atom	X	Y	Z
N	-1.517901	0.008857	-0.391848
C	-2.022982	1.317632	0.006347
H	-1.382299	2.097667	-0.412658
H	-3.034784	1.449659	-0.383310
H	-2.047401	1.432508	1.102340
C	-2.306308	-1.050456	0.237258
H	-3.356041	-0.905560	-0.028889
H	-1.988522	-2.029132	-0.120622
H	-2.211132	-1.020859	1.335676
N	-0.150671	-0.031096	-0.012353
O	0.355205	-1.238859	-0.152207
O	1.996113	1.788392	0.086864
H	1.123879	1.322932	0.059605
H	2.619314	1.035596	0.047704
O	2.980206	-0.876737	-0.058164
H	3.290738	-1.163072	0.814307
H	1.989796	-1.049486	-0.058321

17) Summary NDMA batch reduction experiments in presence and absence of oxygen.

Table S-5. Results of batch NDMA reduction experiment in: a) presence, and b) absence of oxygen. All experiments were carried out in a jacketed divided cell reactor using a rotating disk electrode (RDE) at 25 °C. The initial feed was 150 µM NDMA in all experiments. Cathodic potential for first and second trial in presence of oxygen were -1.12 and -1.47 V/SHE, respectively. Cathodic potential were -1.18 V/SHE for first trial in absence of oxygen, and -1.21 V/SHE for second trial in absence of oxygen.

a)

Sample	Time (min)	Reacted NDMA (µM) – First Trial	DMA Detected (µM) – First Trial	NO_3^- Detected (µM) – First Trial	Reacted NDMA (µM) – Second Trial	DMA Detected (µM) – Second Trial	NO_3^- Detected (µM) – Second Trial
1	15	1.8	< 10	< 5	12.6	11.8	12.3
2	30	5.2	< 10	5.1	14.9	14.4	14.6
3	45	8.2	< 10	7.8	18.2	17.9	17.7
4	60	11.3	10.9	11.1	21.8	21.3	21.5

b)

Sample	Time (min)	Reacted NDMA (µM) – First Trial	DMA Detected (µM) – First Trial	NH_4^+ Detected (µM) – First Trial	NO_3^- Detected (µM) – First Trial	Reacted NDMA (µM) – Second Trial	DMA Detected (µM) – Second Trial	NH_4^+ Detected (µM) – Second Trial	NO_3^- Detected (µM) – Second Trial
1	15	6.2	< 10	5.2	< 5	8.7	< 10	7.5	< 5
2	30	11.7	10.3	8.6	< 5	16.5	15.3	14.6	< 5
3	45	13.3	12.4	10.8	< 5	19.2	17.1	16.2	< 5
4	60	16.5	15.1	13.3	< 5	25.4	22.6	21.1	< 5

References.

(1)   Kedem, S.; Schmidt, J.; Paz, Y.; Cohen, Y. Composite Polymer Nanofibers with Carbon Nanotubes and Titanium Dioxide Particles. *Langmuir* **2005**, *21* (12), 5600–5604.

(2)   Cussler, E. L. *Diffusion: Mass Transfer in Fluid Systems*; Cambridge university press, 2009.

(3)   Nayak, S.; Chaplin, B. P. Fabrication and Characterization of Porous, Conductive, Monolithic Ti$_4$O$_7$ Electrodes. *Electrochim. Acta* **2018**, *263*, 299−310

(4)   Langelier, W. F. The Analytical Control of Anti-Corrosion Water Treatment. *J. Am. Water Works Assoc.* **1936**, *28* (10), 1500–1521.